Stimuli-Responsive Diblock Copolymers by Living Cationic Polymerization: Precision Synthesis and Highly Sensitive Physical Gelation

Shinji Sugihara,[†] Kiyotaka Hashimoto,[‡] Satoshi Okabe,[§] Mitsuhiro Shibayama,[§] Shokyoku Kanaoka,[†] and Sadahito Aoshima*,[†]

Department of Macromolecular Science, Graduate School of Science, Osaka University, Toyonaka, Osaka 560-0043, Japan; Department of Pure and Applied Chemistry, Faculty of Science and Technology, Tokyo University of Science, Noda, Chiba 278-8510, Japan; and Neutron Science Laboratory, Institute for Solid State Physics, The University of Tokyo, Tokai, Ibaraki 319-1106, Japan

Received July 20, 2003; Revised Manuscript Received October 30, 2003

ABSTRACT: Stimuli-responsive diblock copolymers with a thermosensitive segment and a hydrophilic segment have been synthesized via sequential living cationic copolymerization, which involves a poly(vinyl ether) with oxyethylene pendants exhibiting LCST-type phase separation in water and a poly(hydroxyethyl vinyl ether) segment. Highly sensitive and reversible thermally induced micelle formation and/or physical gelation were observed with such diblock copolymers. For example, the flow behavior of an aqueous solution of a diblock copolymer varied from Newtonian to non-Newtonian and plastic flow within a very narrow temperature range. TEM and SANS studies showed that the observed change in viscosity was due to the formation of a macrolattice with body-centered-cubic symmetry of spherical micelles in aqueous solution. The critical temperature of micelle formation and/or physical gelation could be varied by altering the combination of two segments in the diblock copolymer. On the basis of these results, several systems incorporating various patterns of physical gelation behavior have been developed, and a strategy for constructing stimuli-responsive systems with block copolymers was established.

Introduction

Reversible self-assembly of polymers induced by a certain stimulus remains one of the most intriguing issues in polymer science as well as in other fields, including biotechnology and robotics, because it can provide scaffolding for molecular switch systems. Many reports have been published on copolymers that form organized structures in response to an external stimulus such as temperature, pH, light, and chemical addition.[1−7] Reversibility and transition sharpness with such systems can be achieved by utilizing polymers with well-defined primary structures, attainable via living polymerization.

To construct nanoorganized self-assembling polymers including a micelle, diblock copolymers containing two segments with different properties are often employed. A block copolymer with a stimuli-responsive segment would be a powerful tool for constructing reversible self-assemblies. Among poly(vinyl ethers) prepared by living cationic polymerization, those having pendant oxyethylene units exhibit reversible and highly sensitive thermally induced phase separation behavior[8] and are potential stimuli-responsive segments in a block copolymer. Additional advantages of cationic polymerization are the ready availability of various block copolymers with polar functional groups and the ability to easily control molecular weight.

Thus, we synthesized diblock copolymers consisting of a thermosensitive segment and an "always-soluble" segment with well-defined structures. Our preliminary studies showed that an aqueous solution of these diblock copolymers undergoes reversible physical gelation, which may involve organized self-assembly.[9−12] In line with our research on the synthesis of a new family of thermosensitive diblock copolymers, the detailed investigation on the mechanism revealed that the initial association of polymers during gelation is micelle formation, which induces further physical gelation involving macrolattice formation with body-centered-cubic symmetry of spherical micelles.[13,14]

Although similar ordered structures for diblock copolymers in solution have been observed with polystyrene-*b*-polybutadiene (PS−PB)[15−18] or polystyrene-*b*-polyisoprene(PS−PI)[19,20] in organic solvents such as decane, they are less sensitive compared to the diblock copolymers we have developed. In aqueous solutions, various poly(ethylene oxide)-based block copolymers such as poly(ethylene oxide)-*b*-poly(butylene oxide) (PEO−PBO)[21−23] have been systematically examined by many research groups, in which a wide range of techniques have been used to investigate the mechanism and the structure. For example, the effect of block length on the structures of gels has been investigated.[22] However, except for the above-mentioned limited examples, the relationships between polymer structure and sensitivity in transition have been hardly studied systematically because of the difficulty in preparing living copolymers that exhibit stimuli responsiveness. This study establishes a general strategy for realizing reversible self-assembly of diblock copolymers with high sensitivity based on the mechanism we propose. Thus, the precision synthesis of a series of diblock polymers of vinyl ethers having a thermosensitive (**1**−**3**) and a hydrophilic (poly(HOVE)) segment was investigated using an organoaluminum-based initiation system in the presence of an added base (Scheme 1).

[†] Osaka University.
[‡] Tokyo University of Science.
[§] The University of Tokyo.
* To whom correspondence should be addressed. E-mail: aoshima@chem.sci.osaka-u.ac.jp.

10.1021/ma035037t CCC: $27.50 © 2004 American Chemical Society
Published on Web 12/18/2003

Scheme 1

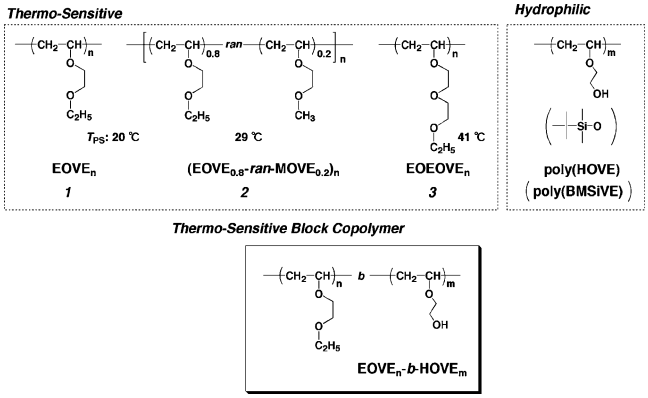

The pathway and gel structure for this thermally induced physical gelation were investigated using analytical techniques such as viscoelastic measurement, dye solubilization, freeze-fracture transmission electron microscopy (FF-TEM), and small-angle neutron scattering (SANS) or small-angle X-ray scattering (SAXS). On the basis of the gelation mechanism confirmed by the study results, we discuss a simple yet generalized strategy for designing stimuli-responsive physical gelation systems.

Experimental Section

Materials. 2-(*tert*-Butyldimethylsilyloxy)ethyl vinyl ether (BMSiVE) and 2-(2-ethoxy)ethoxyethyl vinyl ether (EOEOVE) were prepared as reported previously.[1,2,8,10−12,24] EOVE and MOVE (Maruzen Petrochemical, purity > 98%) were washed with aqueous alkaline solution and then with water. These monomers were purified by double distillation over calcium hydride or sodium (except for BMSiVE) before use (purity > 99% by gas chromatography). Other chemicals were purified by distillation as described as previously reported.[1,8,10,11] All monomers, ethyl acetate, the $Et_{1.5}AlCl_{1.5}$ solution, and IBEA ($CH_3CH(OiBu)OCOCH_3$)[25] were stored in brown ampules under dry nitrogen.

Polymerization Procedures. Polymerization was carried out at 0 °C under a dry nitrogen atmosphere in a glass tube equipped with a three-way stopcock baked at 250 °C for 10 min before use. The reaction was initiated by the addition of an $Et_{1.5}AlCl_{1.5}$ solution in toluene into a mixture of a monomer, ethyl acetate, and the cationogen, IBEA, in toluene at 0 °C by a dry medical syringe. For the example of diblock copolymer, EOVE$_{200}$-*b*-HOVE$_{400}$, after EOVE was polymerized for 4.2 h (condition: $[EOVE]_0 = 0.8$ M, [ethyl acetate] = 1.0 M, $[IBEA]_0 = 4.0$ mM, $[Et_{1.5}AlCl_{1.5}]_0 = 20$ mM in toluene at 0 °C), the second monomer BMSiVE (EOVE/BMSiVE = 1/2 molar ratio) was added at the same temperature. After a certain period (e.g., 48 h for EOVE$_{200}$-*b*-HOVE$_{400}$), the polymerization was quenched with prechilled methanol containing a small amount of aqueous ammonia solution (0.1 wt %). The quenched reaction mixture was diluted with dichloromethane and then washed with water to remove the initiator residues. The product polymer was recovered from the organic layer by evaporation of the solvents under reduced pressure and vacuum-dried overnight. The monomer conversion was determined gravimetrically. Desilylation of the product copolymers was carried out as previously reported.[1]

Polymer Characterization. The molecular weight distribution (MWD) of the copolymers was measured by size exclusion chromatography (SEC) in chloroform at 40 °C on three polystyrene gel columns [TSK gel G-2000H$_{XL}$ (molecular range: $1 \times 10^2 - 1 \times 10^4$ (PSt)), 3000H$_{XL}$ ($6 \times 10^3 - 6 \times 10^4$), and 4000H$_{XL}$ ($1 \times 10^4 - 4 \times 10^5$); 7.8 mm i.d. × 300 mm each; flow rate 1.0 mL/min] connected to a Tosoh DP-8020 dual pump and a RI-8020 refractive detector. The number-average molecular weight (M_n) and M_w/M_n were calculated from SEC curves on the basis of a polystyrene calibration. ^{1}H NMR spectra were recorded on a JEOL JNM-EX270 (270 MHz).

Characterization of Aqueous Copolymer Solutions. Aqueous solutions of the copolymers were prepared by dissolving the polymer in Milli-Q water (18 MΩ cm) and diluting the sample to the desired concentrations. The phase separation temperatures of the solutions were determined from the transmittance at 500 nm through a 1.0 cm quartz sample cell, monitored at a rate of 1.0 °C/min on heating and cooling scans between 5 and 80 °C. The transmittance was recorded on a JASCO V-500 UV/vis spectrometer equipped with a Peltier-type thermostatic cell holder ETC-505.

A high-sensitivity differential scanning calorimeter (DSC8230, Rigaku) was used to study the phase transition. The temperature and heat flow were calibrated using benzoic acid and anisic acid. About 26 mg of polymer samples was placed in a stainless pan (resistance to pressure at 50 atm, 3 × 5 o.d. mm for the vessel size) and then carefully sealed. Thermograms were obtained at the rate of 1.0 °C/min in a heating scan between 10 and 90 °C, with water in another stainless steel pan as a reference.

Rheological Measurement. The (apparent) viscosity and dynamic viscoelasticity of the polymer solutions were measured using a stress-controlled rheometer (Carri-Med CSL^2 100, TA-Instruments). A cone−plate with a diameter of 4 cm and an angle of 2° was employed. In flow property measurements, the shear-stress rate curve was recorded for 3 min while a shear stress was maintained on the sample, and the apparent viscosity was determined from the curve. The storage modulus G' and loss modulus G'' were measured at 40 °C. Depending on the viscoelastic properties, a suitable shear amplitude, γ, was used to ensure the linearity of dynamic viscoelasticity. The dynamic viscoelastic measurement was carried out at varying temperatures with an angular frequency of 6.283 rad/s (1.0 Hz). The temperature was controlled within 0.1 °C by a Peltier element.

Dye Solubilization. A solution of 2,6-diphenyl-1,3,5-hexatriene [DPH (Wako): 5 μL, 10 mM] in THF was added to a 10 mL (DPH: 0.05% v/v) aqueous solution containing various amounts of diblock copolymers. The solution was incubated for at least 30 min in the dark at the desired temperature before UV−vis measurements. The absorbance at 356 nm was recorded from 5 and 80 °C at a rate of 1.0 °C/min on heating by the same spectrometer as that for the measurement of transmittance.

Electron Microscopy. A gel sample (aqueous EOVE$_{200}$-*b*-HOVE$_{400}$) was frozen rapidly in liquid propane using a cryo-preparation apparatus (Leica EM CPC, Leica) and then fractured at −150 °C. The fractured sample surface was coated successively with platinum in about 5 nm thickness and at 45° and carbon in about 10 nm thickness and at 90° by means of sputtering (Freeze Replica Preparing Apparatus, FR-7000A, Hitachi, Ltd.). The metal replica was observed with a transmission electron microscope (JEM-1200EX, JEOL) at an acceleration voltage of 80 kV.

Small-Angle Neutron Scattering (SANS) and Small-Angle X-ray Scattering (SAXS). The SANS experiments were carried out at the SANS-U spectrometer, Institute for Solid State Physics, the University of Tokyo. The wavelength distribution was 13%. The temperature of the sample was regulated with a water circulating bath (NESLAB RTE-111 M). Samples in quartz cells of 1 or 4 mm thick were irradiated by neutron beam for 30 or 60 min depending on the scattering power. The SAXS measurement was carried out with Nano Viewer (Rigaku). The operating condition was 45 kV, at 60 mA, and the beam size was 0.3 × 0.3 mm^2. Monochromatization and intensification were attained with a confocal multilayered mirror optic (Confocal MaxFlux Optic (CMF)). A focused Cu Kα line (wavelength being 1.54 Å) was used for the SAXS measurement.[13,26]

Results and Discussion

Thermally Induced Phase Separation Behavior of Homopolymers and Random Copolymers. The phase separation temperature (T_{PS}) of poly(vinyl ethers) with oxyethylene pendants can be controlled by varying

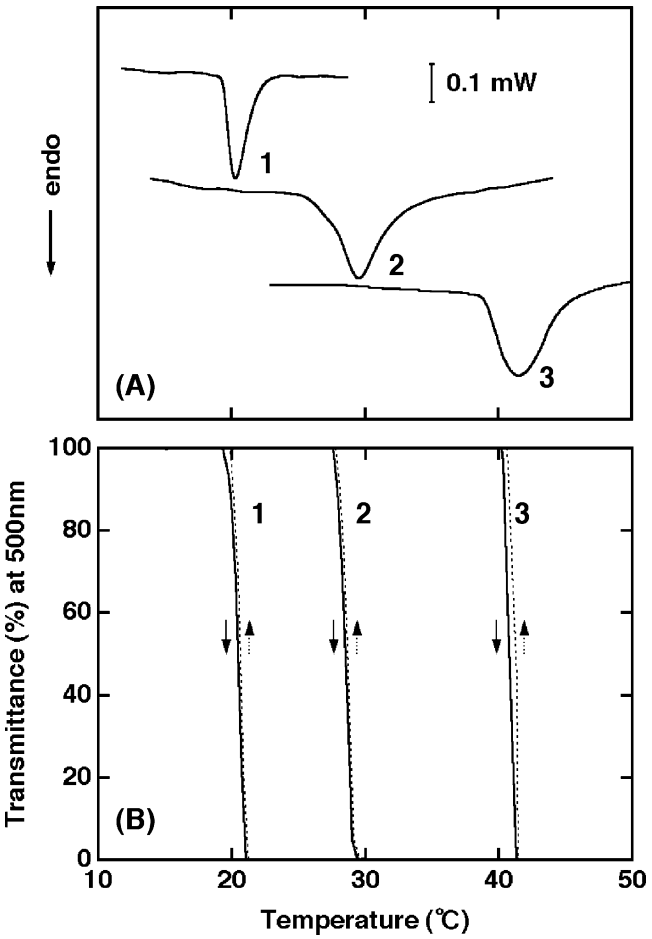

Figure 1. DSC thermograms (A) and temperature dependence of transmittance at 500 nm (B) of 1.0 wt % aqueous solutions of **1**, **2**, and **3** (**1**, $EOVE_{200}$; **2**, $EOVE_{160}$-*ran*-$MOVE_{40}$; **3**, $EOEOVE_{200}$; see Scheme 1 and Table 1 of the structures): rate 1.0 °C/min, heating (—) or cooling (- - -).

the length of the pendant oxyethylene units and/or the hydrophobicity of an ω-alkyl group or by regulating the composition of a random copolymer of two different thermosensitive units, the T_{PS} of which lies between those of two thermosensitive homopolymers.[7−9] Figure 1 shows the temperature dependence of the transmittance at 500 nm and DSC thermograms for aqueous solutions (1.0 wt %) of samples **1**−**3** (see Scheme 1).

The transmittance decreased sharply in all solutions at a specific temperature on heating, indicative of a sharp phase transition (LCST type). This phase separation was not only extremely sensitive but also reversible on heating (solid lines) and cooling (dotted line) without hysteresis. In the DSC thermogram, a single endothermic peak was observed, and the T_{PS} values determined by UV analysis were in good agreement with those from the DSC thermograms (20, 29, and 41 °C for **1**, **2**, and **3**, respectively).

Synthesis of Diblock Copolymers Containing Thermosensitive and Polyalcohol Segments. Sequential block copolymerization of EOVE and BMSiVE was examined using IBEA/$Et_{1.5}AlCl_{1.5}$ in toluene in the presence of ethyl acetate at 0 °C. EOVE was polymerized first, and the monomer BMSiVE was added neat to the polymerization mixture when EOVE had been consumed almost quantitatively. The first stage of polymerization proceeded smoothly without an induction phase to reach 100% conversion in 4.2 h (open circle, Figure 2). After BMSiVE addition, the second

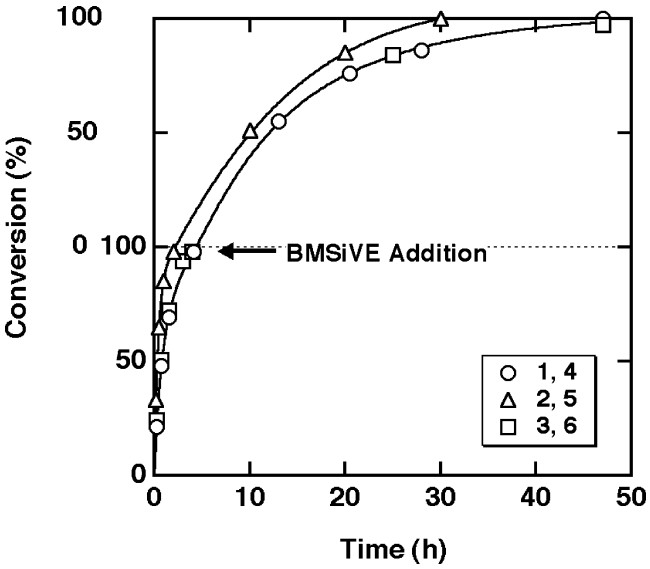

Figure 2. Time−conversion curves for the sequential polymerization of EOVE (for **1**), a mixture of EOVE and MOVE (for **2**), or EOEOVE (for **3**) with BMSiVE (first monomer/BMSiVE = 1/2 molar ratio) (for **4**−**6**) using IBEA/$Et_{1.5}AlCl_{1.5}$ in toluene in the presence of ethyl acetate at 0 °C (see Table 1 for the structures of **1**−**6**): $[monomers]_0$ = 0.8 M ($[EOVE]_0/[MOVE]_0$ = 4/1 for the mixture of EOVE and MOVE), $[IBEA]_0$ = 4.0 mM; $[Et_{1.5}AlCl_{1.5}]_0$ = 20 mM; [added base] = 1.0 M (EOVE = 2-ethoxyethyl vinyl ether; MOVE = 2-methoxyethyl vinyl ether; EOEOVE = 2-(2-ethoxy)ethoxyethyl vinyl ether).

stage of polymerization began immediately and was complete in an additional 45 h. Figure 2 also shows the time−conversion curves in the sequential polymerization of EOEOVE and a mixture of EOVE and MOVE (4:1 molar ratio)[27] with BMSiVE (open triangle and square). In both cases, all monomers were consumed quantitatively to yield soluble polymers having a thermosensitive segment with a T_{PS} different from that of the EOVE homopolymer.

Figure 3 shows the plots of M_n and M_w/M_n of the product polymers as a function of monomer conversion. M_n increased in direct proportion to monomer conversion, and the MWDs of the resulting polymers were very narrow (M_w/M_n < 1.2). After the addition of the second monomer, BMSiVE, M_n increased further in direct proportion to the conversion. The MWDs of the prepared polymers by sequential block copolymerization are shown in Figure 4. In all cases, after monomer addition, the MWDs clearly shifted toward higher molecular weights but still remained very narrow (M_w/M_n < 1.15). In addition, no tailing was observed in the lower molecular weight regions, demonstrating quantitative formation of diblock copolymers and the absence of side reactions that produce homopolymers or oligomers. Composition of the copolymers, as determined by ^1H NMR, agreed with the monomer feed ratios.

The M_n and M_w/M_n of the prepared samples are summarized in Table 1. Entries **1**−**3** are thermosensitive polymers and are prepolymers of **4**−**6**. Entries **4**−**6** are diblock copolymers with a thermosensitive segment and a poly(BMSiVE) segment, which are the precursors of the target diblock copolymers. Entry **7** is a random copolymer with the same composition as **4**. The molecular weight and composition vary in the EOVE−BMSiVE diblock copolymers **8**−**13**. The MWDs of the polymers were invariably narrow, regardless of the monomer combination, molecular weight, or composition.

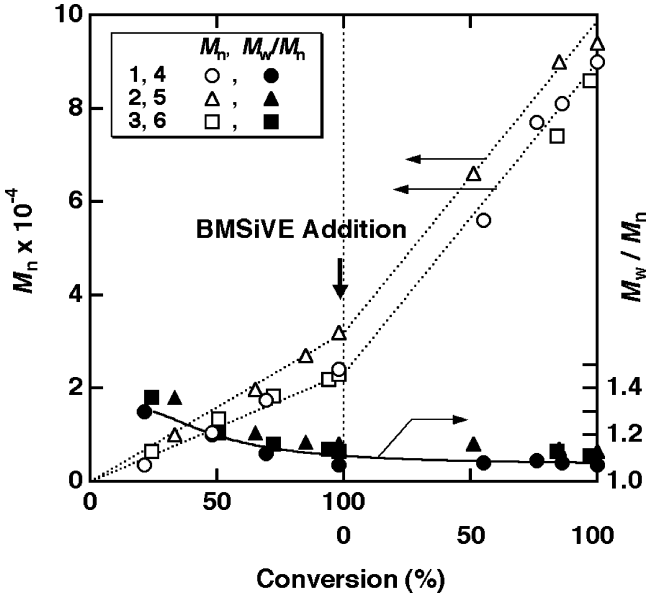

Figure 3. M_n and M_w/M_n of poly(EOVE) (for **1**), poly(EOVE-*ran*-MOVE) (for **2**), or poly(EOEOVE) (for **3**) and diblock copolymers after BMSiVE addition (first monomer/BMSiVE = 1/2 molar ratio) (for **4**−**6**) obtained using IBEA/$Et_{1.5}AlCl_{1.5}$ in toluene in the presence of ethyl acetate at 0 °C (see Table 1 for the structures of **1**−**6**): [monomers]$_0$ = 0.8 M ([EOVE]$_0$/[MOVE]$_0$ = 4/1 for the mixture of EOVE and MOVE), [IBEA]$_0$ = 4.0 mM; [$Et_{1.5}AlCl_{1.5}$]$_0$ = 20 mM; [added base] = 1.0 M (EOVE = 2-ethoxyethyl vinyl ether, MOVE = 2-methoxyethyl vinyl ether, EOEOVE = 2-(2-ethoxy)ethoxyethyl vinyl ether).

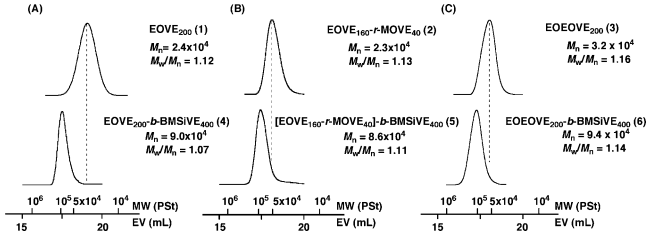

Figure 4. MWD curves of diblock copolymers (**4**−**6**, lower row) and the corresponding thermosensitive polymers (**1**−**3**, upper row) obtained by sequential polymerization of EOVE, a mixture of EOVE and MOVE, or EOEOVE with BMSiVE (see Figures 2 and 3 for the reaction conditions). Prepolymer and block copolymers: (A) **1** and **4**; (B) **2** and **5**; (C) **3** and **6** (see Table 1 for the structures of **1**−**6**).

Desilylation of the copolymers with poly(BMSiVE) segments was conducted using aqueous HCl−EtOH in THF at 0 °C.[1] Quantitative desilylation was confirmed by the disappearance of the ^{1}H NMR signals at 0.1 ppm (s, 6H, Si−CH_3) and 0.9 ppm (s, 9H, Si−C−CH_3) of the *tert*-butyldimethylsilyl group.

Thermally Induced Physical Gelation of Diblock Copolymers. The diblock copolymer $EOVE_{200}$-*b*-$HOVE_{400}$, obtained by the desilylation of **4**, was soluble in water below 20 °C as shown in photograph ***a*** of Figure 5. The solution was a clear liquid with low viscosity (0.155 Pa·s: 20 wt % aqueous solution at 19 °C; Newtonian flow; see Figure 6). When the solution was warmed to 20 °C, gelation occurred rapidly to give a transparent gel. On further heating to 100 °C, the gel remained unchanged, and no syneresis was observed. The gel from a 20 wt % aqueous solution was stiff enough to maintain its shape even when handled with a pair of forceps (photograph ***b*** of Figure 5). When the gel was cooled below 20 °C, it returned to a liquid with almost the same viscosity it had initially, indicating that the gel cross-linking was due to physical interactions, not covalent chemical bonding.

Table 1. Diblock Copolymers and Related Polymers by Sequential Living Cationic Copolymerization

entry	polymer structure[a]	M_n(SEC) × 10^{-4} [b]	M_w/M_n [b]
1	$EOVE_{200}$	2.4	1.12
2	$EOVE_{160}$-*ran*-$MOVE_{40}$	2.3	1.13
3	$EOEOVE_{200}$	3.2	1.16
4	$EOVE_{200}$-*b*-$BMSiVE_{400}$	9.0	1.07
5	($EOVE_{160}$-*ran*-$MOVE_{40}$)-*b*-$BMSiVE_{400}$	8.6	1.11
6	$EOEOVE_{200}$-*b*-$BMSiVE_{400}$	9.4	1.14
7	$EOVE_{200}$-*ran*-$BMSiVE_{400}$	8.4	1.18
8	$EOVE_{200}$-*b*-$BMSiVE_{600}$	12.1	1.21
9	$EOVE_{200}$-*b*-$BMSiVE_{200}$	5.6	1.08
10	$EOVE_{50}$-*b*-$BMSiVE_{550}$	10.1	1.08
11	$EOVE_{100}$-*b*-$BMSiVE_{500}$	9.2	1.09
12	$EOVE_{300}$-*b*-$BMSiVE_{300}$	8.7	1.12
13	$EOVE_{400}$-*b*-$BMSiVE_{200}$	9.0	1.20
14	$EOVE_{500}$-*b*-$BMSiVE_{100}$	7.1	1.21

[a] The segment DP_n in the formula was determined by ^{1}H NMR. The DP_n of initially prepared segments (or homopolymers) was calculated from the feed molar ratio of a monomer and IBEA. [b] By SEC (polystyrene calibration).

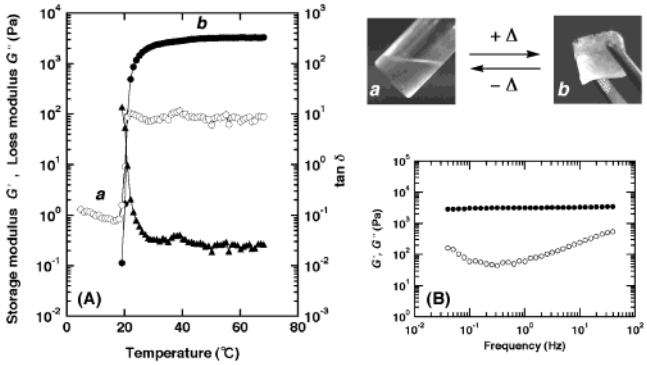

Figure 5. (A) Sol−gel transition of a 20 wt % aqueous solution of $EOVE_{200}$-*b*-$HOVE_{400}$ monitored by dynamic viscoelasticity measurement (frequency = 1 Hz). Storage modulus G' (●), loss modulus G'' (○), and tan δ (▲). (B) Frequency dependence of dynamic moduli, G' (●) and G'' (○), of aqueous $EOVE_{200}$-*b*-$HOVE_{400}$ at 40 °C: [polymer] = 20 wt %. The photographs show the aqueous solution at (a) 15 °C and (b) 40 °C.

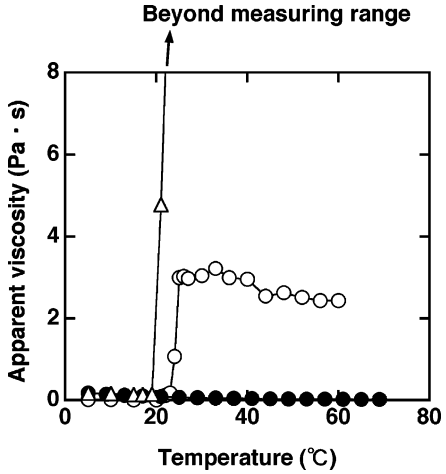

Figure 6. Temperature dependence of apparent viscosity for 20 wt % $EOVE_{200}$-*b*-$HOVE_{400}$ (△), 5.0 wt % $EOVE_{200}$-*b*-$HOVE_{400}$ (○), and 20 wt % $EOVE_{200}$-*ran*-$HOVE_{400}$ (●) aqueous solutions (shear rate: 10 s^{-1}).

The dynamic viscoelasticity of an aqueous $EOVE_{200}$-*b*-$HOVE_{400}$ solution (20 wt %) was measured at a fixed angular frequency (1.0 Hz) and is consistent with the

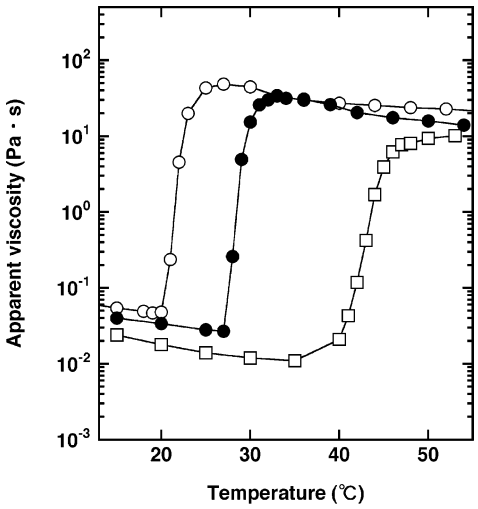

Figure 7. Temperature dependence of apparent viscosity for 10 wt % $EOVE_{200}$-*b*-$HOVE_{400}$ (○), ($EOVE_{160}$-*ran*-$MOVE_{40}$)-*b*-$HOVE_{400}$ (●), and $EOEOVE_{200}$-*b*-$HOVE_{400}$ (□) aqueous solutions (shear rate: 10 s^{-1}).

change in state shown in the photographs in Figure 5. At temperatures below 20 °C, the solution behaved as a liquid with a loss modulus G'' much larger than the storage modulus G', which was not even detectable ($G'' \gg G'$). Upon heating, G' increased sharply ca. 4 orders of magnitude and became at least 20 times larger than G'' ($G' \gg G''$) above 20 °C. Figure 5B is a double-logarithmic plot of G' at 40 °C against frequency for the sample obtained from a 20 wt % aqueous solution of $EOVE_{200}$-*b*-$HOVE_{400}$. There is an almost horizontal plateau over a wide range of frequencies, with G'' considerably smaller than G' in the plateau region, results consistent with the behavior of a typical gel.

Figure 6 shows the apparent viscosity, which was defined as a given shear stress divided by shear rate (10 s^{-1}), as a function of temperature. The apparent viscosity above 20 °C increased beyond that of the solution, even at a lower polymer concentration (5.0 wt %). An increase of 0.014 Pa·s (Newtonian flow) to 3.0 Pa·s (non-Newtonian flow) occurred as the temperature was raised from 18 to 22 °C. This implies that polymer assemblies (micelles) with apparent larger molecular weights begin forming slightly below the T_{PS}.

With a 20 wt % aqueous solution, viscosity increased significantly and exceeded the measuring range of the rheometer employed here above 21 °C because of the stiffness of the gel. Flow behavior varied from Newtonian flow (<20 °C) to non-Newtonian and plastic flow (≥20 °C) within a very narrow temperature range. The drastic change in flow behavior indicates that polymer chains aggregate rapidly at the critical temperature of the thermosensitive segment before physical gelation. In contrast to diblock copolymers, a random copolymer, entry **7**, with the same molecular weight and composition as the diblock copolymer, exhibited no increase in apparent viscosity with temperature, even at higher concentrations (Figure 6).

Figure 7 compares the temperature dependence of apparent viscosity (shear rate, 10 s^{-1}) for 10 wt % aqueous solutions of diblock copolymers (see Table 1 for the corresponding precursors, entries **4**−**6**) having different thermosensitive segments with different T_{PS} values (see Figure 1). Irrespective of the structure of the thermosensitive segment, gelation occurred in a manner similar to that of $EOVE_{200}$-*b*-$HOVE_{400}$, except

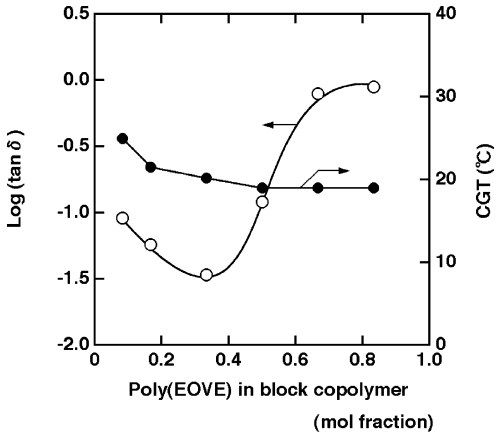

Figure 8. Relationship between logarithm of tan δ or CGT (critical gelation temperature) and the composition of diblock copolymers ($EOVE_x$-*b*-$HOVE_{600-x}$) in water at 20 wt %.

for the critical temperature. Thus, gelation temperature can be controlled by the structure of thermosensitive segments. These results also indicate that the association of the thermosensitive moiety is a driving force for thermally induced physical gelation.

Effects of the Composition of $EOVE_n$-*b*-$HOVE_m$. In general, composition of the diblock copolymers significantly influences the ordered structure in solution.[20,22,28,29] Thus, the effects of composition and length of the hydrophilic segment of $EOVE_n$-*b*-$HOVE_m$ on physical gelation were investigated. With the DP_n of EOVE fixed at a 200-mer, the length of the HOVE segment was varied (see Table 1 for the corresponding precursors, entries **8** and **9**). In both cases, thermally induced physical gelation occurred above 20 °C of T_{PS} for poly(EOVE). The gel obtained from a 10 wt % aqueous solution of $EOVE_{200}$-*b*-$HOVE_{200}$, (23.1 Pa·s at 30 °C (shear rate, 10 s^{-1})), however, was slightly opaque and was softer than that of $EOVE_{200}$-*b*-$HOVE_{400}$. The apparent viscosity (shear rate, 10 s^{-1}) at 30 °C was smaller with $EOVE_{200}$-*b*-$HOVE_{600}$ (34.4 Pa·s) than with $EOVE_{200}$-*b*-$HOVE_{400}$ (44.5 Pa·s), although the molecular weight of $EOVE_{200}$-*b*-$HOVE_{600}$ is larger than that of $EOVE_{200}$-*b*-$HOVE_{400}$.

The effects of composition on physical gelation were further examined for polymers with total $DP_n = 600$. Figure 8 shows the plots of the loss tangent ($\tan \delta = G''/G'$) at 30 °C and the critical gelation temperature (cgt: the temperature at $G' = G''$) against the mole fraction of EOVE in $EOVE_x$-*b*-$HOVE_{600-x}$ (mole fraction: x/600) for a 20 wt % aqueous solution (see Figure 5 for measurement conditions). In the case of shorter poly(EOVE), the cgt increased slightly, since the T_{PS} values of homopolymers of EOVE increase as their molecular weight decreases.[8,11] The tan δ, which is a measure for the stiffness of a gel, reached a minimum when mole fraction was approximately 0.3−0.4, indicating that the stiffest gel was obtained at this point.

Pathway for Physical Gelation. (a) Micellization. A water-insoluble dye, DPH, becomes soluble in water when surrounded by a hydrophobic environment; hence, it can be used for the determination of critical micelle concentration (cmc) and temperature (cmt).[11,30−32] To determine whether micelles form in a transient state, the absorbance of DPH in a solution of $EOVE_{200}$-*b*-$HOVE_{400}$ (10^{-5}−10^{-2} g/mL) was monitored by UV−vis spectrometry. The dotted line in Figure 9A shows a typical UV−vis absorption spectrum of a solution of

Table 2. The cmc, cmt, and cgt of Thermosensitive Diblock Copolymers

polymer structure	cmc[a] (g/mL)	cmt (°C)[a] (5×10^{-3} g/mL)	cgt (°C)[b] (15 wt %)
$EOVE_{200}$-*b*-$HOVE_{400}$	6.3×10^{-4} (30 °C)	19.4	20.5
($EOVE_{160}$-*ran*-$MOVE_{40}$)-*b*-$HOVE_{400}$	5.5×10^{-4} (40 °C)	28.0	28.5
$EOEOVE_{200}$-*b*-$HOVE_{400}$	5.0×10^{-4} (50 °C)	41.3	41.5

[a] Determined by solubilization of DPH. [b] By dynamic visoelastic measurement.

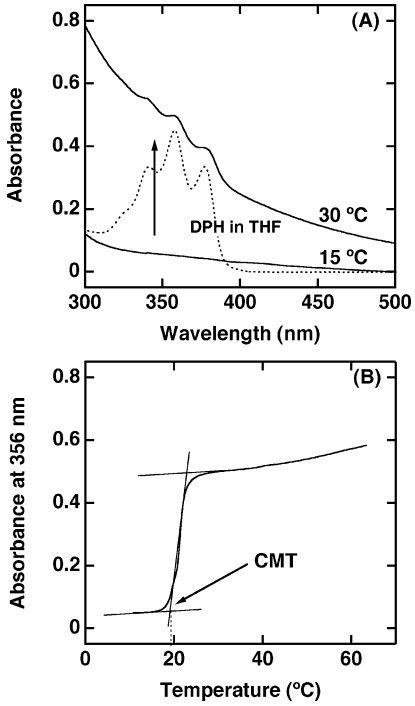

Figure 9. (A) UV−vis absorption spectra of DPH (5 μM) in a 5.0×10^{-3} g/mL of $EOVE_{200}$-*b*-$HOVE_{400}$ aqueous solution at 15 and 30 °C. The dotted line is an absorption of DPH (5 μM) in neat THF at 30 °C. (B) Absorption intensity at 356 nm for DPH (5 μM) in a 5.0×10^{-3} g/mL of $EOVE_{200}$-*b*-$HOVE_{400}$ aqueous solution as a function of temperature. Heating rate: 1.0 °C/min.

DPH (5 μM) in THF, with characteristic absorptions at 341, 356, and 377 nm. In the presence of $EOVE_{200}$-*b*-$HOVE_{400}$ (5.0×10^{-3} g/mL) in water, no absorption peaks of DPH were observed at 15 °C. At 30 °C, peaks assignable to DPH appeared, supporting the formation of micelles of the diblock copolymer.

Figure 9B shows the plot of absorption intensity at 356 nm as a function of temperature. The cmc and cmt of various concentrations were determined from the first inflection of the absorption intensity at 356 nm, plotted against temperature. For an aqueous solution of $EOVE_{200}$-*b*-$HOVE_{400}$, the cmc and cmt were 6.3×10^{-4} g/mL and 19.4 °C (polymer concentration, 5.0×10^{-3} g/mL), respectively. The cmc value was relatively smaller than those of the common surfactants and PEO-based triblock copolymers such as PEO-*b*-PPO-*b*-PEO [PEO: poly(ethylene oxide), PPO: poly(propylene oxide)].[31,33] The cmc and cmt values of various diblock copolymers are summarized in Table 2. No differences between cmt and cgt existed. These results support the formation of micelles in a transient state between the disorder (molecular dispersion in solution) and order (in gel) structures and indicate that gelation occurs immediately after micelles are generated near the T_{PS}.

(b) Physical Gelation. Figure 10 shows a TEM picture of a freeze fracture replica of a physical gel prepared from a 20 wt % aqueous $EOVE_{200}$-*b*-$HOVE_{400}$ solution at 40 °C. The gel sample prepared at 40 °C was rapidly frozen in liquid propane, preserving the morphology, and then fractured at −150 °C. Spherical aggregates were densely packed across the field of view, which is direct evidence that an ordered structure of micelles is responsible for the physical gelation.

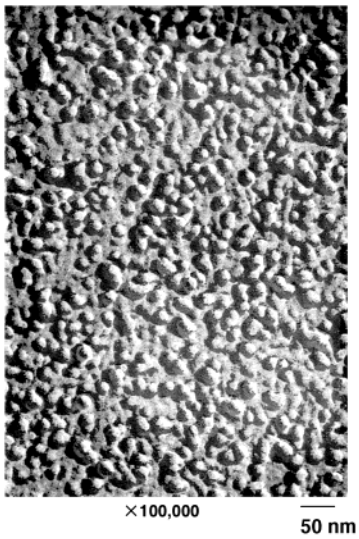

Figure 10. FF-TEM image for a gel obtained from an aqueous 20 wt % $EOVE_{200}$-*b*-$HOVE_{400}$ solution at 40 °C.

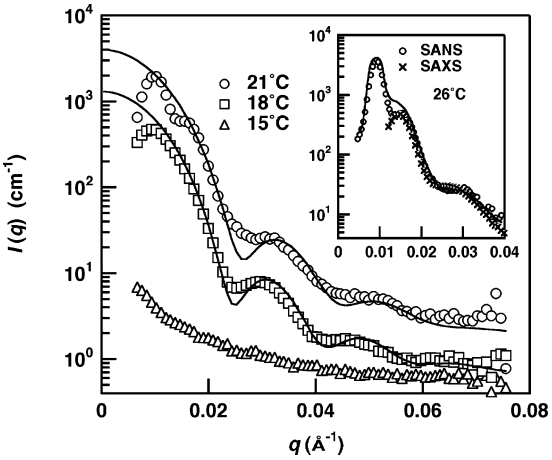

Figure 11. SANS scattering intensity curves for 17 wt % $EOVE_{200}$-*b*-$HOVE_{400}$ in D_2O at 15 °C (△), 18 °C (□), and 21 °C (○) and results of curve fit of the SANS scattering intensity functions with the equation in ref 39. The inset shows the SANS (○) and SAXS (×) scattering intensity curves for 17 wt % $EOVE_{200}$-*b*-$HOVE_{400}$ in D_2O at 26 °C and the result of curve fit of the scattering intensity function with Hosemann−Bagchi's paracrystal theory.[40]

As mentioned in the Introduction, SANS[13] and dynamic light scattering[14] studies showed that physical gelation is due to the formation of a macrolattice of spherical micelles in aqueous solution. Thus, SANS and SAXS scattering measurements were performed with a 17 wt % aqueous $EOVE_{200}$-*b*-$HOVE_{400}$ solution at 15, 18, and 21 °C. The solid lines in Figure 11 represent curve fittings for the data at 18 and 21 °C. Polymer

Scheme 2

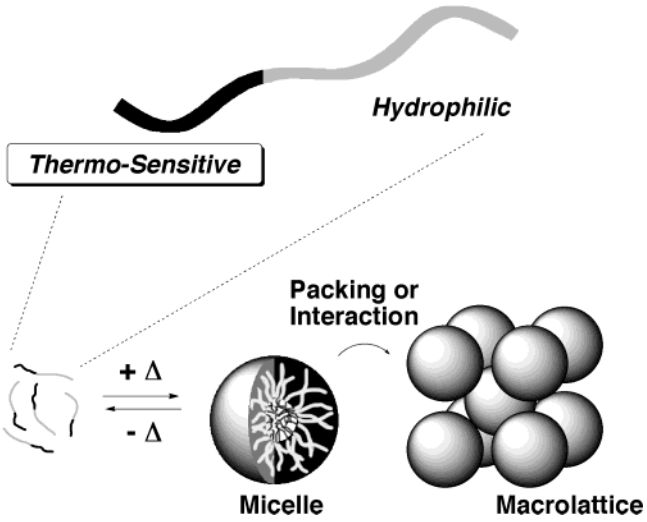

concentration was high enough to induce physical gelation.

With increasing temperature, scattering peaks appeared, and the curves fit the spherical particle function. A peak at the small scattering vector appeared at 21 °C due to macrolattice formation. The peak also fits the Hosemann−Bagchi's paracrystal theory (see Figure 11 inset) as well as the lattice factor for a body-centered-cubic (bcc) lattice, indicating that the diblock copolymers in a disordered state in solution (15 °C) transformed into spherical micelles (18 °C) and finally formed a macrolattice (bcc) near 21 °C (Scheme 2). In the micelle region, the size of the core and number of diblock chains were 180−200 Å and 633, respectively. The average radius of the poly(EOVE) domain and its distribution were constant at various concentrations.

Stimuli-Responsive Physical Gelation Behavior. We have demonstrated that physical gelation starts with the formation of spherical micelles, which are induced by the insolubilization of a thermosensitive segment as illustrated in Scheme 2. Subsequent macrolattice formation transforms the solution into a gel. Judging from this gelation mechanism, diblock copolymers and their analogues that contain a stimuli-responsive segment would induce similar physical gelation. On the basis of this concept, we have developed several highly sensitive self-assembling systems.[34] Scheme 3 shows schematic illustrations of physical gelation behavior for a series of block copolymers, which have typical segments that are divided into three categories: hydrophilic (group A), thermosensitive (group B), and hydrophobic chains (group C).

In contrast to the diblock copolymers already discussed, a combination of B and C produces physical gelation in aqueous solution[35] or organic solvent[36] with decreasing temperature (pattern ***b***). Interestingly, diblock[1,10,11] or triblock[37] copolymers having multiple thermosensitive segments with differing T_{PS} values exhibit self-assembly behavior with multistage transitions (patterns ***c*** and ***d***), placing them into a novel class of stimuli-responsive copolymers. Furthermore, similar gelation involving macrolattice formation occurs with diblock copolymers of C with A or B under a stimulus such as the addition of a selective solvent or a compound (pattern ***e***).[5,38]

Scheme 3. Schematic Illustrations of Various Patterns of Physical Gelation Behavior for a Series of Block Copolymers

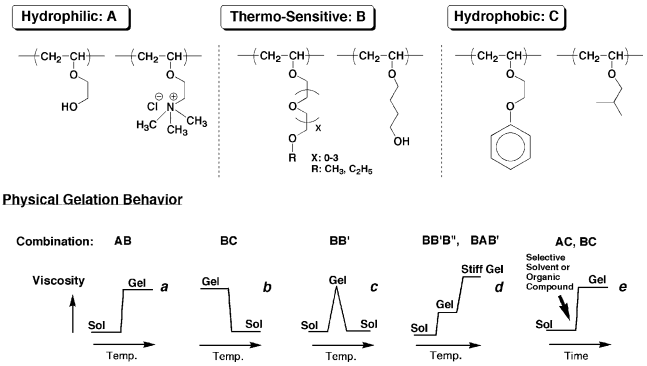

Conclusion

Stimuli-responsive block copolymers were prepared by sequential living cationic polymerization using the IBEA/$Et_{1.5}AlCl_{1.5}$ initiating system in toluene in the presence of ethyl acetate at 0 °C. This study not only demonstrates the effects of polymer sequence, concentration, composition, and structure on thermally induced micellization but also reveals the mechanism of the physical gelation. To realize thermosensitive physical gelation, the total DP_n and composition of block copolymers must be chosen to produce a spherical micelle. This study provides a solid foundation for further development of various stimuli-responsive self-assembling systems using block copolymers.

Acknowledgment. This study was supported in part by a grant for "The development of the basic technologies for the industry system construction harmonized with environment" promoted by Shiga Prefecture under the program of Collaboration of Regional Entities for the Advancement of Technological Excellence by Japan Science and Technology Corp. We express our special thanks for the center of excellence (21COE) program "Creation of Integrated EcoChemistry" of Osaka University. We also thank Prof. M. Abe and Dr. H. Sakai of the Department of Pure and Applied Chemistry, Faculty of Science and Technology, Tokyo University of Science, for the viscoelasticity measurement.

References and Notes

(1) Sugihara, S.; Hashimoto, K.; Matsumoto, Y.; Kanaoka, S.; Aoshima, S. *J. Polym. Sci., Part A: Polym. Chem.* **2003**, *41*, 3300.
(2) Sugihara, S.; Kanaoka, S.; Aoshima, S. *Macromolecules*, submitted.
(3) *Stimuli-Responsive Water Soluble and Amphiphilic Polymers*; McCormick, C. L., Ed.; ACS Symposium Series 780; Oxford: New York, 2000.
(4) Hoffman, A. S. *Macromol. Symp.* **1995**, *98*, 645.
(5) Sugihara, S.; Matsuzono, S.; Sakai, H.; Abe, M.; Aoshima, S. *J. Polym. Sci., Part A: Polym. Chem.* **2001**, *39*, 3190.
(6) Aoshima, S.; Sugihara, S. *J. Jpn. Oil Chem. Soc.* **2000**, *49*, 1061.
(7) Aoshima, S.; Kobayashi, E. *Macromol. Symp.* **1995**, *95*, 91.
(8) Aoshima, S.; Oda, H.; Kobayashi, E. *J. Polym. Sci., Part A: Polym. Chem.* **1992**, *30*, 2407.
(9) Aoshima, S.; Oda, H.; Kobayashi, E. *Kobunshi Ronbunshu* **1992**, *49*, 937.
(10) Aoshima, S.; Sugihara, S. *J. Polym. Sci., Part A: Polym. Chem.* **2000**, *38*, 3962.
(11) Sugihara. S.; Aoshima, S. *Kobunshi Ronbunshu* **2001**, *58*, 304.
(12) Aoshima, S.; Hashimoto, K. *J. Polym. Sci., Part A: Polym. Chem.* **2001**, *39*, 746.

(13) Okabe, S.; Sugihara, S.; Aoshima, S.; Shibayama, M. *Macromolecules* **2002**, *35*, 8139.
(14) Okabe, S.; Sugihara, S.; Aoshima, S.; Shibayama, M. *Macromolecules* **2003**, *36*, 4099.
(15) Watanabe, H.; Kotaka, T.; Hashimoto, T.; Shibayama, M.; Kawai, H. *J. Rheol.* **1982**, *26*, 153.
(16) Shibayama, M.; Hashimoto, T.; Kawai, H. *Macromolecules* **1983**, *16*, 16.
(17) Hashimoto, T.; Shibayama, M.; Kawai, H.; Watanabe, H.; Kotaka, T. *Macromolecules* **1983**, *16*, 361.
(18) Hashimoto, T.; Shibayama, M.; Kawai, H. *Macromolecules* **1983**, *16*, 1093.
(19) Gast, A. P. *Langmuir* **1996**, *12*, 4060.
(20) McConnell, G. A.; Gast, A. P.; Huang, J. S.; Smith, S. D. *Phys. Rev. Lett.* **1993**, *71*, 2102.
(21) Booth, C.; Yu, G.-E.; Nace, V. M. In *Amphiphilic Block Copolymers: Self-Assembly and Applications*; Alexandridis, P., Lindman, B., Eds.; Elsevier: Amsterdam, 1997.
(22) Hamley, I. W.; Mai, S.-M.; Ryan, A. J.; Fairclough, J. P. A.; Booth, C. *Phys. Chem. Chem. Phys.* **2001**, *3*, 2972.
(23) Li, H.; Yu, G.-E.; Price, C.; Booth, C.; Hecht, E.; Hoffmann, H. *Macromolecules* **1997**, *30*, 1347.
(24) Higashimura, T.; Ebara, K.; Aoshima, S. *J. Polym. Sci., Part A: Polym. Chem.* **1989**, *27*, 2937.
(25) Aoshima, S.; Higashimura, T. *Macromolecules* **1989**, *22*, 1009.
(26) Shibayama, M.; Okabe, S.; Nagao, M.; Sugihara, S.; Aoshima, S.; Harada, T.; Matsuoka, H. *Macromol. Res.* **2002**, *10*, 311.
(27) The monomer reactivity ratios, r_{EOVE} and r_{MOVE}, determined by the Fineman−Ross method were 1.00 and 1.07, respectively, indicative of the occurrence of ideal copolymerization to yield random copolymers.[7]
(28) Zhang, L.; Eisenberg, A. *Science* **1995**, *268*, 1728.
(29) As a review, see: Hamley, I. W. *The Physics of Block Copolymers*; Oxford Science: New York, 1998.
(30) Chattopadhyay, A.; London, E. *Anal. Biochem.* **1984**, *139*, 408.
(31) Alexandridis, P.; Holzwarth, J. F.; Hatton, T. A. *Macromolecules* **1994**, *27*, 2414.
(32) Forder, C.; Patrickios, C. S.; Armes, S. P.; Billingham, N. C. *Macromolecules* **1996**, *29*, 8160.
(33) Tuzar, Z.; Kratochvil, P. In *Surface and Colloid Science*; Matijevic, E., Ed.; Plenum Press: New York, 1993; Vol. 15, p 1.
(34) Aoshima, S.; Sugihara, S.; Shibayama, M.; Kanaoka, S. *Macromol. Symp.*, submitted.
(35) For example, the increase in viscosity was observed with a 20 wt % aqueous solution of $PhOVE_{200}$-*b*-$MOVE_{400}$ (PhOVE: 2-phenoxyethyl vinyl ether) as the temperature was decreased: $G' = 670.3 > G'' = 96.7$ (Pa) at 20 °C (gel), $G' = G'' = 18.4$ (Pa) at 44 °C (critical temperature), and $G' = 8.7 < G'' = 13.0$ (Pa) at 47 °C (sol). Aoshima, S.; Sugihara, S.; Hashimoto, K.; Matsuzono, S. *Polym. Prepr., Jpn.* **1999**, *48*, 2084.
(36) By utilizing a segment exhibiting UCST-type phase separation in an organic solvents, the transition pattern opposite to that in this study was also observed. For example, the increase in viscosity was observed with 25 wt % decane solution of $IBVE_{300}$-*b*-$EOVE_{300}$ (IBVE: isobutyl vinyl ether) as the temperature was decrease: $G' = 2210.0 > G'' = 131.0$ (Pa) at 20 °C (gel), $G' = G'' = 244.5$ (Pa) at 27.4 °C (critical temperature), and $G' = 0.059 < G'' = 8.8$ (Pa) at 30 °C (sol). Aoshima, S.; Inaoka, M.; Yoshida, T.; Sugihara, S.; Kanaoka, S. *Polym. Prepr., Jpn.* **2002**, *51*, 1297.
(37) For example, the increase in viscosity was observed with 20 wt % aqueous solution of $EOVE_{200}$-*b*-$MOVE_{200}$-*b*-$EOEOVE_{200}$ as the temperature was increased (apparent viscosity at 10 s^{-1}): 0.084 (Pa·s) at 18 °C (sol), 10.5 (Pa·s) at 23 °C (gel), and beyond measuring range over 41 °C (stiff gel). (a) Sugihara, S.; Kanaoka, S.; Aoshima, S. *J. Polym. Sci., Part A: Polym. Chem.*, submitted. (b) Aoshima, S.; Sugihara, S.; Kobayashi, E. *Polym. Prepr., Jpn.* **1998**, *47*, 1297.
(38) Fuse, C.; Okabe, S.; Shibayama, M.; Sugihara, S.; Aoshima, S. *Polym. Prepr., Jpn.* **2003**, *52*, 655.
(39) The fitting curves were obtained by $I_{R+\lambda}(q)$,[13] is given in the following form: $I_{R+\lambda}(q) = (w/d_p)\Delta\rho^2[(\int\int W_R(R)W_\lambda(\lambda)V^2(R)\Phi^2(qR)\,dR\,d\lambda)/(\int\int W_R(R)W_\lambda(\lambda)V(R)\,dR\,d\lambda)]$, where w, d_p, $\Delta\rho$, R, λ, and V are polymer concentration, mass density, scattering length density difference between the sphere and matrix, radius of the sphere, the wavelength of the incident beam, and the volume of sphere. The size distribution, $W_R(R)$, was assumed to be a Gaussian function. $\Phi^2(q)$ is the form factor for a sphere.
(40) Figure 11 inset shows the result of curve fitting with the paracrystal theory as well as the calculated lattice factor for bcc lattice.[13] The open circles denote the SANS data obtained with an extended camera length of 8 m for $EOVE_{200}$-*b*-$HOVE_{400}$ at 17 wt % at 26 °C. The solid line denoted the curve-fitted result of the case with $g = 0.1$, called the Hosemann's g factor, and 970 Å of the unit cell distance by taking account of the smearing of the incident beam width and the wavelength distribution.

MA035037T